SUPPLEMENTARY FIGURES

Figure S1
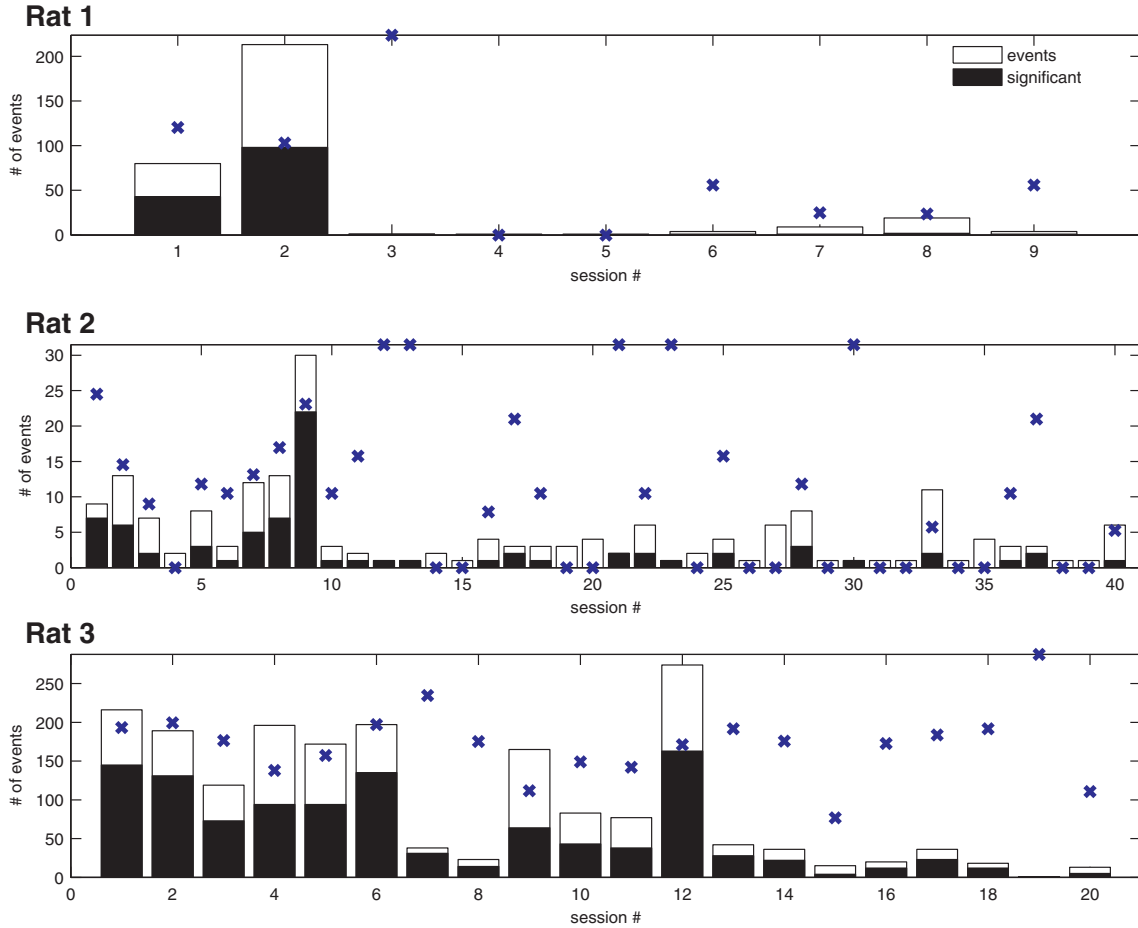
Sequence events as a function of experience. Bar plots, for each rat, show the number of all detected events for each recording session. The black part of each bar indicates the significant fraction. Only sessions yielding at least one event were considered. Blue x's indicate the ratio of significant to total events, scaled by the length of the y-axis. Note the constant ratio across sessions and the decreasing number of events with experience (sessions).

Figure S2

place field sequence
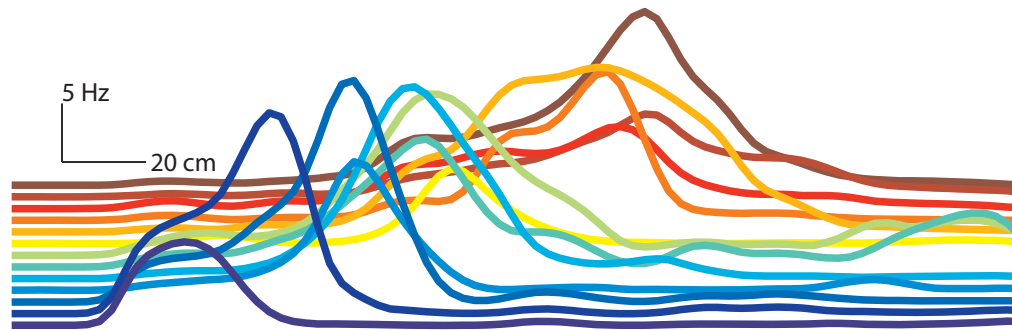
Illustration of place-field sequence "template" and examples of forward and reverse replay sequences. Top panel shows a series of neuronal place-fields, (the same ones depicted in main text Fig. 1a) which, when ordered according to the peak in-field firing rates, comprise the place-field sequence "template". Each neuron's place-field is shown in a different color. Bottom panel shows some sample forward and reverse correlated events from these neurons (same coloring) during immobility.

Figure S3
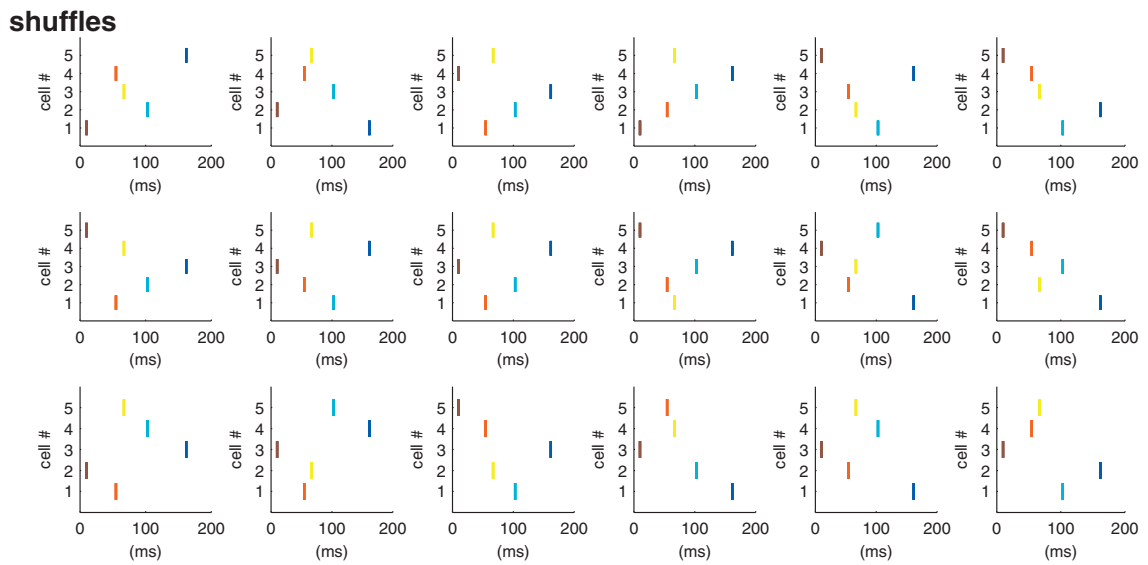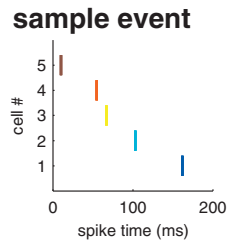
Illustration of the shuffling procedure. A sample event is shown on top, depicting the first spikes from 5 different neurons. 18 example shuffled surrogate events are shown below, for which cell identities were shuffled across spikes.

Figure S4

time of events
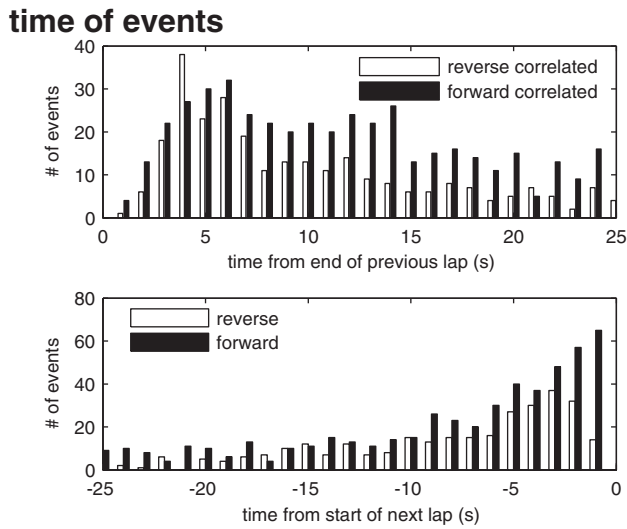
Pre-play (forward) events increase prior to run. This figure explores the timing of forward and reverse correlated events relative to the onset (below) and end (above) of lap running. The time spent in the reward area following the end of lap running is quite variable. Consequently, there is no clear asymptote to the rate of events following a lap, though a gradual rise in events occurs within seconds. On the other hand, forward correlated events steadily rise prior to the onset of a lap, along with a drop in the rate of occurrence of reverse correlated events during the last two seconds.

Figure S5

sample CCG's
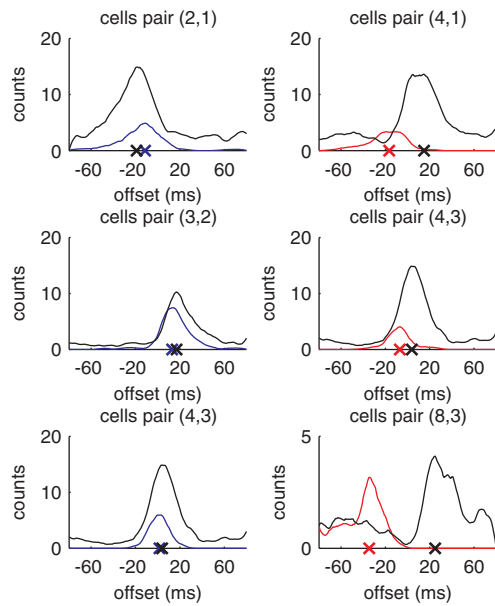
Temporal order between neuron pairs. Left panels show cross-correlograms calculated for neuron pairs across forward correlated events (blue) and across track running epochs (black; 'theta compression''). Colored x's on the abscissa indicate the time-offsets of the peaks. Right panels show similar cross-correlograms calculated for reverse correlated events (red) and during running on the track (black). These time offsets between peaks during running and immobility were used to construct Fig. 2c.

Figure S6
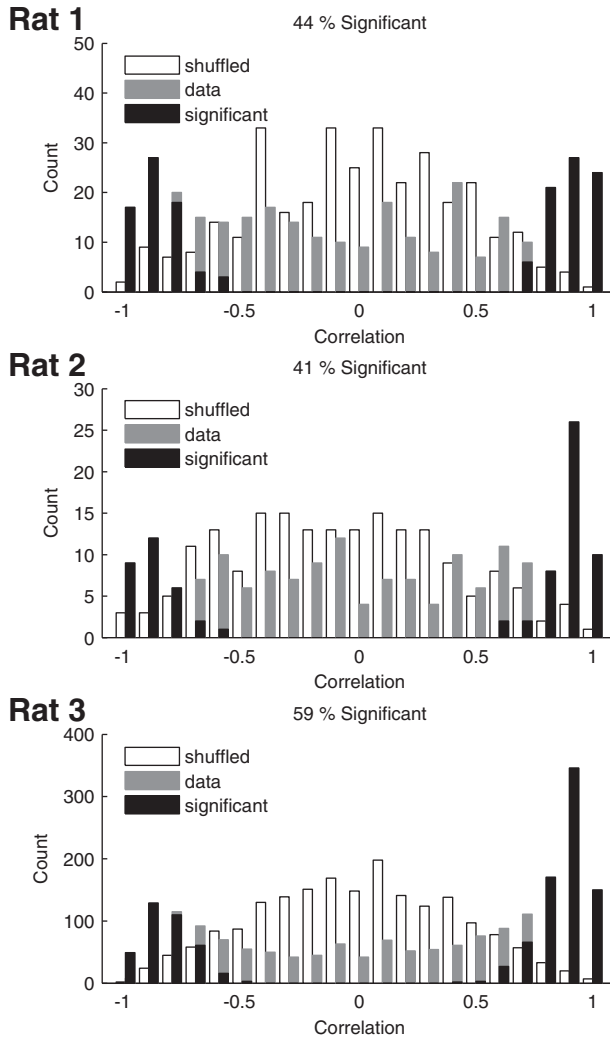
Within-subject analysis. Histograms show rank-order correlations of the immobility sequences, and an equal number of shuffled surrogate events, to the place-field run sequence template, calculated for each rat separately. Significantly forward and reverse correlated events (black) were detected for each animal.

Figure S7
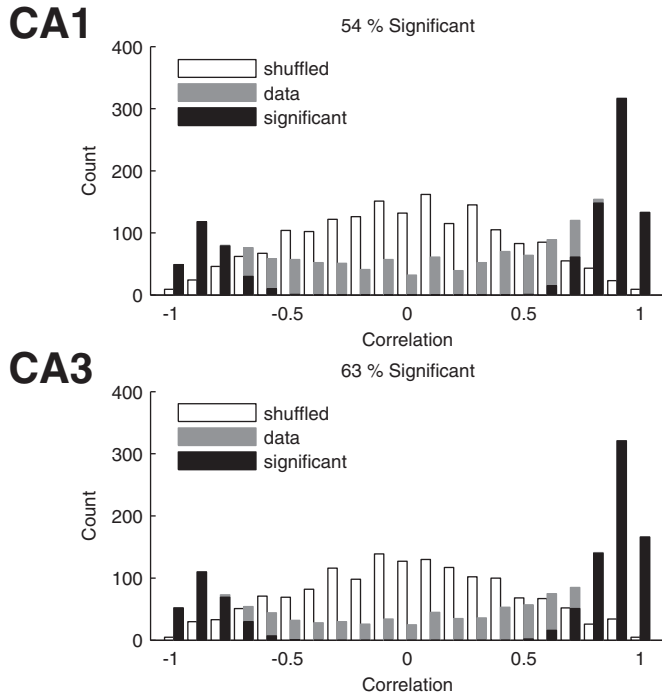
Pre-play and replay sequences occur in both CA1 and CA3 regions. Histograms show rank-order correlations of the immobility sequences, and an equal number of shuffled surrogate events, to the place-field run sequence template, calculated for CA1 and CA3 subfields by considering only events for which ≥ 4 neurons from the subfield fired. Significantly forward and reverse correlated events (highlighted) were detected for each hippocampal subfield.

Figure S8
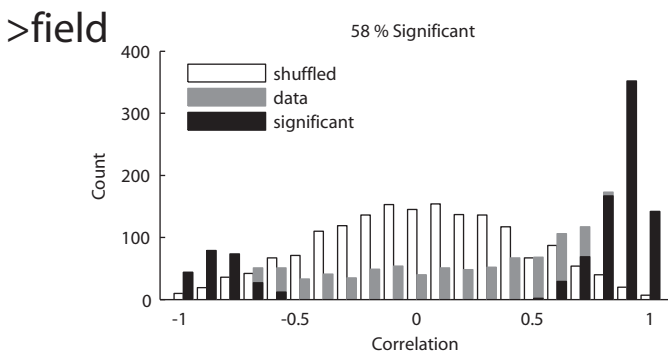
Place field proximity cannot account for the forward or reverse sequences. Histograms show rank-order correlations of the immobility sequences, and an equal number of shuffled surrogate events, to the place-field run sequence template, calculated for considering only events for which ≥ 4 neurons fired ≥ 10 cm outside of the boundaries of their place-fields (defined by 95 percent of the peak firing, see text). Significantly forward and reverse correlated events (black) were nevertheless detected.

Figure S9
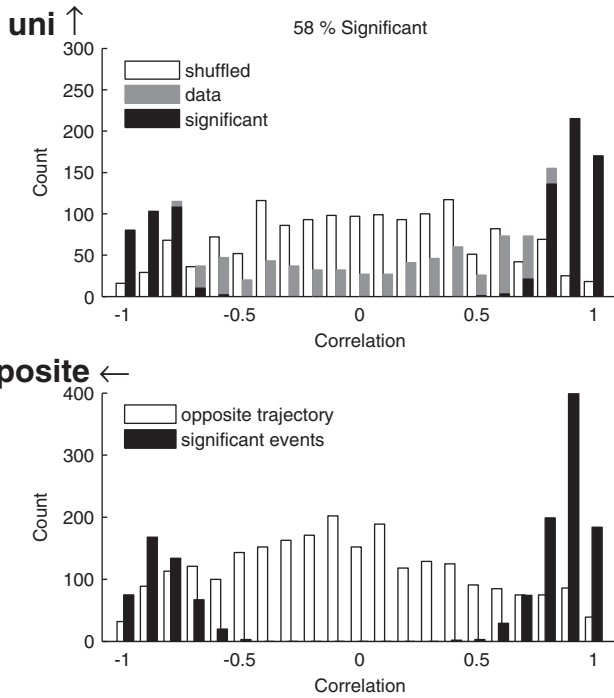
Bidirectional place cells cannot account for the forward or reverse sequences. Top panel: histograms show rank-order correlations of the immobility sequences, and an equal number of shuffled surrogate events, to the place-field run sequence template, calculated when considering only events for which ? 4 unidirectional place-cells fired. A place-cell was considered unidirectional if its peak firing rate was ? 4 times (and ? 5 Hz) in one trajectory. Bottom panel: we correlated all significant events to templates created by the same neurons, but in the opposite trajectory regardless of peak firing rate (i.e. with no lower threshold—therefore even a few spikes could define the template). These histograms show that bidirectional cells do not explain the forward pre-play and reverse replay we observed.

Figure S10
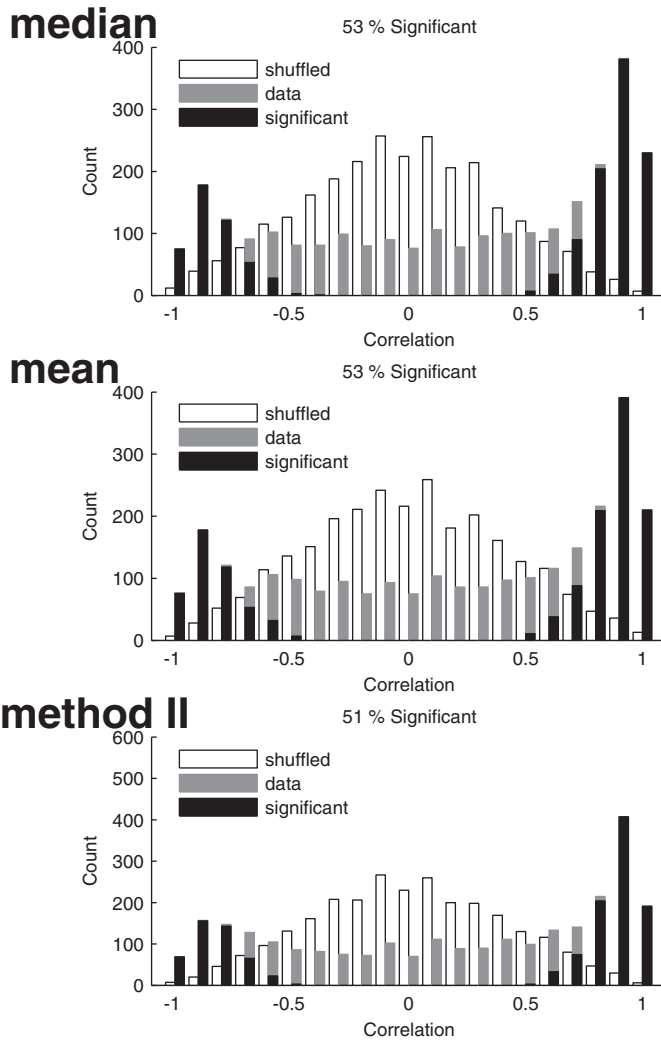
Significant pre- and replay event are detected independent of the sampling methods. Histograms show rank-order correlations of the immobility sequences, and an equal number of shuffled surrogate events, to the place-field run sequence template, calculated using the median and mean spikes (instead of the 1st spike) from each cell. Results were not altered in either case. Bottom panel presents an alternative shuffling algorithm, whereby the ordering of cells in the sequence template is permuted and shuffled correlations are calculated from the shuffled templates on the track, rather than from shuffled events during immobility. This method yielded a similar result.

Figure S11
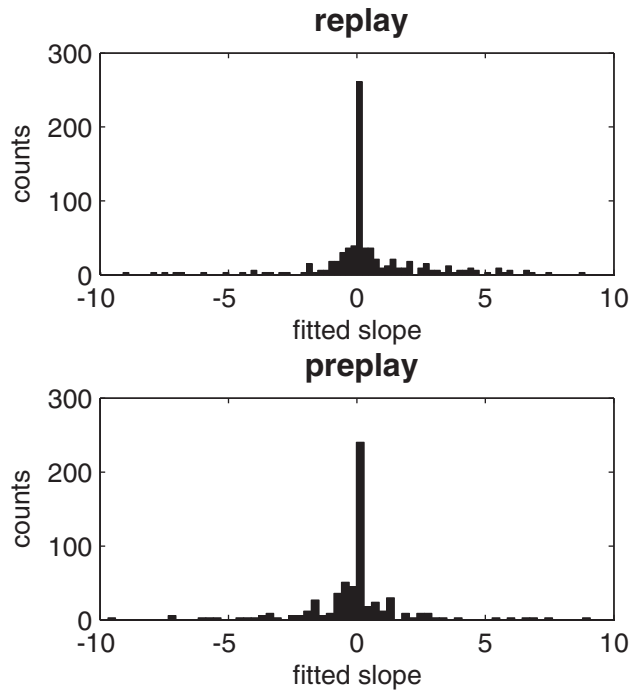
Excitability of place cells alone cannot explain the forward vs. reverse order of sequences. The number of pre-play and replay events for each neuron was fitted against the number of spikes it fired during running in the previous (replay) or following (pre-play) lap, to test if transient excitation of neurons on the track could determine their participation in immobility events.

Figure S12
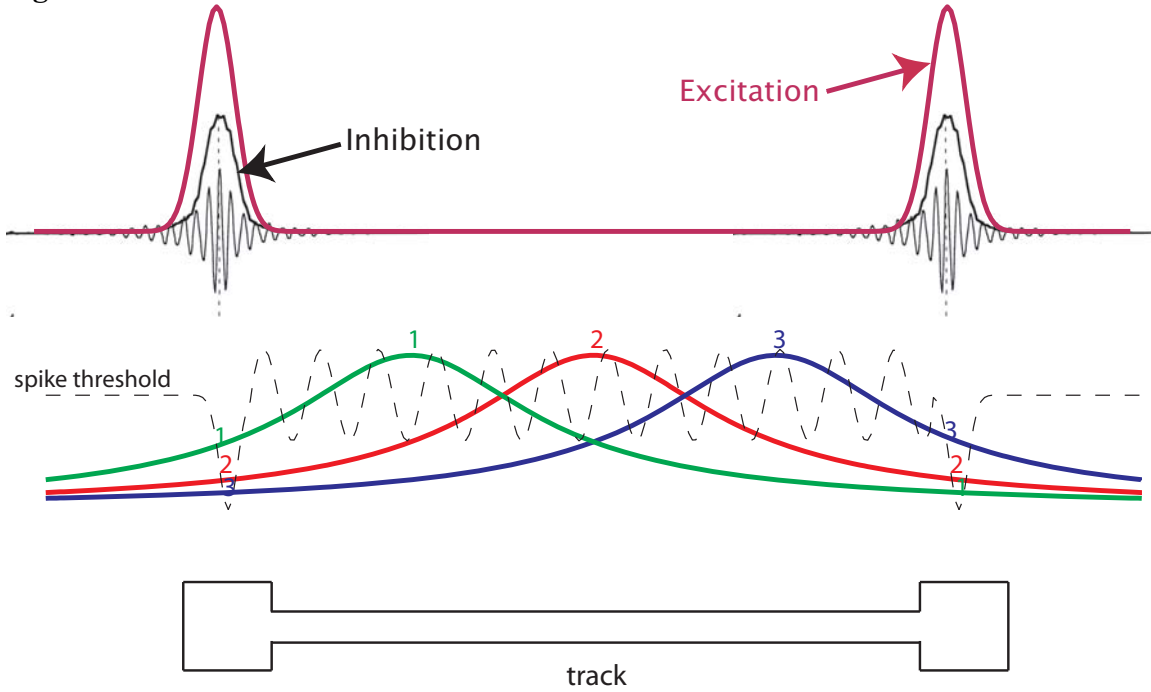
A hypothetical place-field model may account for sequences observed during both pre-play and replay. Inputs for three neurons are indicated in color. A global spiking threshold is shown with a dashed line. On the track, this threshold is theta-modulated, resulting in phase-precession (Harris et al., 2002; Mehta et al., 2002). On the platforms, during immobility, a transient decrease in the global threshold causes cells to fire outside of their classical place-fields. Furthermore, the sequence of firing is forward or reverse correlated to the place-field sequence, according to the platform end of the track where the rat is. The top panel illustrates the transient rise in global excitation (and inhibition), deduced from population spiking activity, during immobility ripples (Csicsvari et al., 1999a).

Forward and reverse hippocampal place cell sequences during ripples

Kamran Diba and György Buzsáki

Center for Molecular and Behavioral Neurobiology, Rutgers University, 197 University Ave, Newark, NJ 07102, E-mails: diba@.rutgers.edu, buzsaki@axon.rutgers.edu, Telephone: (973)353-1080 ext. 3361, Fax:(973)353-1820.

SUPPLEMENTARY RESULTS

Results were combined from all 3 animals in the main text (**Fig. 1**). However, significant results were also obtained for each animal considered separately (**Fig. S6**).

CA1 and CA3 regions. Units from both CA1 and CA3 participated in the pre-play and replay events. We did not observe any differential trends in their firing and pooled all cells for analysis. Limiting the significance analysis to only CA3 or only CA1 units gave similar results to the pooled results presented in this report (**Fig. S7**)

Place-field "tails". Csicsvari et al. (in press) have argued that reverse replay, as observed by Foster and Wilson (2006), could arise as a consequence of the "tail" of place-fields. The tuning curve of a place-field falls with increasing distance from the peak-firing location (i.e. the place-field "center"). Csicsvari et al. (in press) defined the 95 percent boundary of a place-field by the location of a 95 percent drop in its mean firing rate; then, they showed that as long as the animal is within this boundary for a given place-field, the cell will fire in inverse relation to the distance from the place-field center during sharp wave-ripple complexes, thereby representing a potential mechanism for reverse replay. We tested this hypothesis on our dataset by including only those cells for which the rat was ≥ 10 cm outside of their 95 percent peak boundaries, at the instantaneous position. Yet, we found that the remaining cells were sufficient to display significant forward pre-play and reverse replay (**Fig. S8**), indicating that the persistent, place-controlled firing of neurons alone cannot explain the results in this manuscript.

Inclusion of bidirectional cells. Only a fraction (21 percent) of the cells included for analysis was bi-directional, i.e. fired ≥ 5 Hz on both left and right trajectories. Since events were detected separately for each trajectory template, it was possible for a bidirectional cell to contribute to both pre-play forward events and replay reverse events. If an event was detected twice (446 such events), it was assigned to the trajectory with the greater number of participating cells, or else, the template with the stronger correlation. The strong correlation of the forward or reverse events with the animals' location, as illustrated in **Fig. 1c**, could only be weakened by the ambiguity introduced with bidirectional cells; hence their inclusion underlines the strength of our results. Nevertheless, we tested whether significant events could be detected if we removed these cells, keeping only cells whose peak firing was at least 4 times higher in one direction than the other. Still, significant results were observed (top panel, **Fig. S9**). We also looked at the correlation of the "significant" events, from **Fig. 1b**, to the peak firing place-field sequence template based on the opposite trajectory (left vs. right), with no lower limit on the firing rate. Such a template can therefore be defined even if the cells fire only one or two spikes on the opposite trajectory. The results (bottom panel, **Fig. S9**) indicate that the bidirectionality of a fraction of cells

cannot explain the correlations we observed.

Alternative methods. We experimented with using the median or the mean spike, instead of the first spike, in calculating the rank-order correlations between the event sequences and the place-field sequences. Results did not differ appreciably (top two panels, **Fig. S10**), demonstrating that pre-play and replay are robust events. We also tested an alternative shuffling algorithm, whereby instead of shuffling each event 500 times to obtain 500 surrogate events, we shuffled the place-field sequence 500 times to obtain alternate template sequences. Thus, events were deemed significant if the correlation (either positive or negative) with the place-field sequence was greater than for 95 percent of the shuffled template sequences. These results were also consistent with our main conclusion (bottom panel, **Fig. S10**).

The impact of training on sequence replay. Foster and Wilson (2006) reported that reverse replay was more robust in a novel as opposed to a familiar environment. To examine the impact of training, we plotted the number of detected sequences as a function of session number (**Fig. S1**). We observed that in early sessions, the rat spent more time in immobility (and emitted more ripples) in the reward areas compared with later, over-trained sessions. Consequently, many more sequences were detected than in later sessions. However, the ratio of significant events to recorded events appeared to be roughly constant, regardless of the session number (**Fig. S1**).

Potential mechanisms

Firing rate during run vs. probability of spiking during pre-play and replay. One hypothesis for the reverse replay is that some hypothetical neuromodulator in expectation of reward (e.g., dopamine, Foster and Wilson, 2006) or the intense firing during the run transiently changes the intrinsic properties of neurons leading to their increased excitability. Within this framework, the main difference between pre-play and replay is that the latter is preceded by intense spiking activity of the neurons. This may, in principle, bring about a transient enhancement of excitability. In **Figure S11**, we plot a histogram of the best linear fits between the number of times a cell participated in a significant forward or reverse event, and the number of spikes it fired in the upcoming or previous run, respectively. The lack of correlation between firing rate during run and probability of discharge during either replay or pre-play sequences in the same trials fail to support the idea that this mechanism alone can account for the reverse replay. It is also renders unlikely the hypothesis that pre-play and replay events are directly affected by the intrinsic excitability of the neurons.

An alternative to changes in the intrinsic properties of active place cells (Foster and Wilson, 2006), short-term modification of synaptic circuitry may be at play (Buzsaki, 1989). Following intense spiking activity of pyramidal cells, the pyramidal-perisomatic interneuron synapse undergoes transient depotentiation (Ali and Thomson, 1998; Markram et al., 2004; Pouille and Scanziani, 2004; Silberberg and Markram, 2007). This use-dependent decrease of recurrent inhibition (or "disinhibition") may selectively enhance the excitability of recently active place cells; place neurons that were active during later parts of the run can produce stronger disinhibition compared to place neurons active in the earlier parts. Such a mechanism can account for reverse replay during sharp waves, when inhibition is 2 to 3 times less efficient than during theta oscillations (Csicsvari et al., 1998; Csicsvari et al., 1999a), thus favoring the discharge of a larger proportion of neurons. Pre-play and replay

of (sharp wave-related) sequences may help bring about bidirectional alteration in a randomly connected CA3 recurrent collateral system. Such a high-dimensional interconnected matrix can support large numbers of activity trajectories that are determined by hypothesized attractor dynamics (McNaughton et al., 1996; Tsodyks, 2005; Wills et al., 2005). Depending on the 'seed' at the time of sharp waves, the activity trajectory may therefore move either forward or backward: reverse replay occurs when triggered by use-dependent disinhibition of recently active neurons, forward pre-play occurs when the animal is anticipating a behaviorally established trajectory. This hypothesis could also account for the observation that forward (pre-play) sequences show a stronger similarity to run related sequences, compared to reverse (replay) events (**Fig. 2b**,**c**).

A variation of this hypothesis is that the interplay between environmental and internal events determines the exact trajectory of activity (i.e., a cell assembly sequence). The assumption here is that the hypothetical subthreshold place fields of neurons are considerably larger than those characterized by their observed (supra-threshold) place-fields. That is to say, cells with firing fields on the track receive subthreshold input in the reward areas, away from their place-fields. A model of this scenario is shown in **Fig. S12**. When the global spike threshold of the entire population of cells is decreased transiently, as occurs during sharp wave ripples (Csicsvari et al., 1999a), the activity spreads according to the excitability of the neurons. Prior to the run, this activity observes the same sequence as that expressed by the place field firing during theta-associated running, whereas after the run, the sharp wave-related decrease of the spike threshold brings about an activity sequence in the reverse order. A similar model was proposed to account for the asymmetric expansion of place-fields (Mehta et al., 2000; Mehta, 2001; Mehta et al., 2002) and to explain the dual rate and time code of phase-precessing CA1 neurons (Harris et al., 2002; Mehta et al., 2002).

SUPPLEMENTARY METHODS

We trained three male Sprague-Dawley rats (335 - 400 g) to run back and forth on a linear track (79 cm, 125 cm, and 170 cm length, 6.2 cm width) for water reward at both ends (end platforms 21 x 21 cm2). After learning the task, the rats were implanted with 32 and/or 64-site silicon probes in the left dorsal hippocampus under isoflurane anesthesia. The silicon probes, consisting of 4 or 8 individual shanks (spaced 200 μm apart) of 8 staggered recording sites (20 μm spacing) (Csicsvari et al., 2003), were lowered to CA1 and CA3 pyramidal cell layers. Following recovery from surgery (~ 1 week) we tested the animals again on the track. All protocols were approved by the Institutional Animal Care and Use Committee of Rutgers University. We continuously recorded all channels at 32552 Hz over the following 7-10 days with a 128-channel DigitaLynx recording system (Neuralynx, Bozeman, MT). We obtained the local field potential (LFP) from each channel by low-pass filtering up to 1252 Hz. The position was tracked with an LED and later linearized along the axis of the track. After recording, we high-pass filtered the data (0.8-16 kHz), and thresholded for spike detection, assisted by freely available ND manager software (http://ndmanager.sourceforge.net; Hazan et al., 2006). For each putative spike, we sampled 54 data points at each of the 8 recording sites on the shank, centered on the maximum spike amplitude. Based on the resulting set of 54 dimensional vectors, we calculated three principal components for each recording site. We clustered these 24 principal components using previously described methods (http://klustakwik.sourceforge.net; Harris et al., 2000) with the freely available Klusters

program (http://klusters.sourceforge.net; Hazan et al., 2006). We separated pyramidal cells and interneurons on the basis of their auto-correlograms, waveforms and mean firing rates (Csicsvari et al., 1999a), using freely available Neuroscope software (http://neuroscope.sourceforge.net; Hazan et al., 2006). Well-isolated pyramidal cells with stable single place-fields of peak ≥ 5 Hz on the track (on either or both of the left to right, and the right to left trajectories) were utilized in subsequent analysis (1256 out of 6491 clusters, averaging 18.2 ± 6.8 per session, 69 sessions in all: 9 sessions in Rat 1, 40 sessions in rat 2, and 20 sessions in rat 3; see **Fig. S1**). The majority of these cells (989 out of 1256) were unidirectional (fired only on left to right, or right to left journeys).

A trajectory was marked when the animal left one reward area platform, traversed the track, and entered the other reward area platform. The locations of the peak firing of neurons in each trajectory (left vs. right) were generally stable from trial to trial (about 20 trials of each trajectory per session). Peak in-field firing locations, calculated over the entire session, defined a place-field sequence template (average 9.1 members) for each trajectory (**Fig. S2**, top panel). Data were subsequently analyzed with MATLAB (Mathworks, Natick, MA) for each of the two templates separately. Pre-play and replay sequences were collected only when the animal was in one of the two track-end reward areas. After quickly drinking the water reward (in < 1 second), the amount of time animals spent in these areas, pacing, sniffing, whisking, grooming, or remaining stationary, was variable across trials and sessions, and appeared to be related to their (difficult to ascertain) motivation level. Animals spent approximately 82 percent of the time in the reward areas. When the animal's speed was ≤ 10 cm s$_{-1}$ (~'immobility'; about 77 percent of the time spent in reward areas), pre-play/replay events were detected by searching for silent periods ≥ 60 ms. If ≥ 5 or ≥ 30 percent of place-cells (whichever was greater) from a template fired within the next 300 ms, an event was recorded. We constructed a sequence for each event, based on the first spike-time of each cell within the 300 ms window (mean and median spike-times gave similar results; **Fig. S10**). We determined the rank-order correlation between these event sequences and the corresponding place-field sequence templates. For each event, we constructed 500 shuffled surrogate events by randomizing the cell identity of the spikes; this effectively results in a randomized sequence (**Fig. S3**). Events were considered significant if they were more positively (forward) or negatively (reverse) correlated to the place-field sequence than 95 percent of the shuffled events. In principle, pre-play (prior to lap run) and replay (following lap run) of either trajectory sequence, in either a forward or a reverse correlated manner, could occur in the reward areas on both sides of the track. However, data presented in the main text demonstrated a bias for forward correlated events during pre-play and reverse correlated events during replay. The p-values were then calculated for the number of observed significant events based on a binomial distribution of probability = 0.05. Ninety-five percent confidence intervals on the ratio of forward to reverse events were calculated using the cumulative binomial distribution function for a range of probability ratios and taking only those that were within null range. In all, 2450 events were recorded in 3 animals, yielding up to 274 events in a single session (**Fig. S1**). The number of recorded events per session was highly variable (averaging 19 events per session, or 0.1 events per second of immobility), and largely contingent on the amount of time the animal spent immobile in the reward areas, the amount of training, and the number of place-fields recorded in that session. **Figure S4** illustrates the time distribution of significant events in the reward area, relative to the end or beginning of a lap run.

Ripples detection was previously described (Csicsvari et al., 1999b). First, by band-pass

filtering the local field potential from a recording site in the CA1 pyramidal layer the root-mean-square power was calculated in the 100-300 Hz ripple-band; ripples were detected when a threshold of 2 standard deviations (SDs) above the mean was exceeded. Onset of ripples was marked at the point when the ripple power was at 1.5 SDs above the mean. Cross-correlations were calculated, for main text **Fig. 2a**, between the onset (first spike) of significant forward and reverse correlated events, and the onset of the ripple events. We detected about 0.2 ripples per second in the reward areas (roughly twice the rate of pre/replay events).

Cross-correlograms (CCGs) were constructed for pairs of neurons during pre-play, replay, and track running (**Fig. S5**). All spikes fired during significantly forward and reverse correlated events, and all spikes fired during track running were used. CCGs were binned (1 ms) and smoothed (over 8 bins). Only pairs with CCGs containing a single peak ≥ 2 counts were used in the analysis (main text **Figs 2b**,**c**).

Ali AB, Thomson AM (1998) Facilitating pyramid to horizontal oriens-alveus interneurone inputs: dual intracellular recordings in slices of rat hippocampus. J Physiol 507 (Pt 1):185-199.

Buzsaki G (1989) Two-stage model of memory trace formation: a role for "noisy" brain states. Neuroscience 31:551-570.

Csicsvari J, Hirase H, Czurko A, Buzsaki G (1998) Reliability and state dependence of pyramidal cell-interneuron synapses in the hippocampus: an ensemble approach in the behaving rat. Neuron 21:179-189.

Csicsvari J, O'Neill J, Allen K, Senior T (in press) Eur J Neurosci.

Csicsvari J, Hirase H, Czurko A, Mamiya A, Buzsaki G (1999a) Oscillatory coupling of hippocampal pyramidal cells and interneurons in the behaving Rat. J Neurosci 19:274-287.

Csicsvari J, Hirase H, Czurko A, Mamiya A, Buzsaki G (1999b) Fast network oscillations in the hippocampal CA1 region of the behaving rat. J Neurosci 19:RC20.

Csicsvari J, Henze DA, Jamieson B, Harris KD, Sirota A, Bartho P, Wise KD, Buzsaki G (2003) Massively parallel recording of unit and local field potentials with silicon-based electrodes. J Neurophysiol 90:1314-1323.

Foster DJ, Wilson MA (2006) Reverse replay of behavioural sequences in hippocampal place cells during the awake state. Nature 440:680-683.

Harris KD, Henze DA, Csicsvari J, Hirase H, Buzsaki G (2000) Accuracy of tetrode spike separation as determined by simultaneous intracellular and extracellular measurements. J Neurophysiol 84:401-414.

Harris KD, Henze DA, Hirase H, Leinekugel X, Dragoi G, Czurko A, Buzsaki G (2002) Spike train dynamics predicts theta-related phase precession in hippocampal pyramidal cells. Nature 417:738-741.

Hazan L, Zugaro M, Buzsaki G (2006) Klusters, NeuroScope, NDManager: a free software suite for neurophysiological data processing and visualization. J Neurosci Methods 155:207-216.

Markram H, Toledo-Rodriguez M, Wang Y, Gupta A, Silberberg G, Wu C (2004) Interneurons of the neocortical inhibitory system. Nat Rev Neurosci 5:793-807.

McNaughton BL, Barnes CA, Gerrard JL, Gothard K, Jung MW, Knierim JJ, Kudrimoti H, Qin Y, Skaggs WE, Suster M, Weaver KL (1996) Deciphering the hippocampal polyglot: the hippocampus as a path integration system. J Exp Biol 199 (Pt 1):173-185.

Mehta MR (2001) Neuronal dynamics of predictive coding. Neuroscientist 7:490-495.

Mehta MR, Quirk MC, Wilson MA (2000) Experience-dependent asymmetric shape of hippocampal receptive fields. Neuron 25:707-715.

Mehta MR, Lee AK, Wilson MA (2002) Role of experience and oscillations in transforming a rate code into a temporal code. Nature 417:741-746.

Pouille F, Scanziani M (2004) Routing of spike series by dynamic circuits in the hippocampus. Nature 429:717-723.

Silberberg G, Markram H (2007) Disynaptic inhibition between neocortical pyramidal cells mediated by Martinotti cells. Neuron 53:735-746.

Tsodyks M (2005) Attractor neural networks and spatial maps in hippocampus. Neuron 48:168-169.

Wills TJ, Lever C, Cacucci F, Burgess N, O'Keefe J (2005) Attractor dynamics in the hippocampal representation of the local environment. Science 308:873-876